

Deep Reinforcement Learning-based Quadcopter Controller: A Practical Approach and Experiments

Truong-Dong Do¹, Nguyen Xuan-Mung² and Sung-Kyung Hong^{3*}

¹Department of Aerospace System Engineering, Sejong University,
Seoul, 05006, South Korea (¹dongdo@sju.ac.kr)

^{1,3}Department of Convergence Engineering for Intelligent Drone, Sejong University,
Seoul, 05006, South Korea (³skhong@sejong.ac.kr)

^{2,3}Faculty of Mechanical and Aerospace Engineering, Sejong University,
Seoul, 05006, South Korea (²xuanmung@sejong.ac.kr) * Corresponding author

Abstract: Quadcopters have been studied for decades thanks to their maneuverability and capability of operating in a variety of circumstances. However, quadcopters suffer from dynamical nonlinearity, actuator saturation, as well as sensor noise that make it challenging and time consuming to obtain accurate dynamic models and achieve satisfactory control performance. Fortunately, deep reinforcement learning came and has shown significant potential in system modelling and control of autonomous multicopter aerial vehicles, with recent advancements in deployment, performance enhancement, and generalization. In this paper, an end-to-end deep reinforcement learning-based controller for quadcopters is proposed that is secure for real-world implementation, data-efficient, and free of human gain adjustments. First, a novel actor-critic-based architecture is designed to map the robot states directly to the motor outputs. Then, a quadcopter dynamics-based simulator was devised to facilitate the training of the controller policy. Finally, the trained policy is deployed on a real Crazyflie nano quadrotor platform, without any additional fine-tuning process. Experimental results show that the quadcopter exhibits satisfactory performance as it tracks a given complicated trajectory, which demonstrates the effectiveness and feasibility of the proposed method and signifies its capability in filling the simulation-to-reality gap.

Keywords: deep reinforcement learning, quadcopter controller, end-to-end, sim2real, and actor-critic network.

1. INTRODUCTION

Unmanned aerial vehicles (UAVs), in particular quadrotors, are increasingly prevalent research subjects due to their flexibility and autonomy [1–3]. With hovering capabilities and vertical take-off and landing (VTOL), a plethora of applications including search and rescue, infrastructure assessment, and urban air mobility [4, 5]. Precision and agility in flying movements are essential in these applications. The dynamics of quadrotors are highly nonlinear and often hard to model specific system, which presents a considerable challenge in terms of stabilization control. Conventional cascaded hierarchy controls require domain expertise and engineering to be adjusted for changing hardware and utilization circumstances. Moreover, this method often takes extensive setup and experiment time, along with parameter optimization [6, 7].

Recent developments in machine learning and deep learning have proven efficient in addressing various complicated problems [8, 9]. Robot control is a decision-making problem that can be characterized as a Markov Decision Process (MDP), in contrast to supervised learning, in which labels tend to be not directly exist. In order to deal with MDPs, reinforcement learning has been utilized to train policies for complicated end-to-end control problems in simulation [10–12]. Additionally, they demonstrate encouraging results in learning tasks involving continuous state/action space [10], which have a close relationship to quadrotor control [13]. Compared with typical optimization methods, this technique eliminates

the necessity for a specified controller structure, which might constrain agent performance and increase human effort. Despite results achieved in simulation are incredible, the reality gap between simulation and real-world systems is a notable challenge to the deployment of trained control policies. This is essentially due to model imperfections, inaccurate state observations, uncertainty from observation and action, and other disturbances [14, 15].

In this research, an end-to-end reinforcement learning based quadcopter controller is proposed to deal with the aforementioned problems. The aim is to create a controller that is extremely data efficient, free of human gain adjustments, and is safe for real-world implementation. First, a novel actor-critic-based architecture is designed to directly translate quadcopter states to motor Revolutions Per Minute (RPM) outputs without any supplementary pre-configured controllers. Then, a python simulated environment was created using OpenAI Gym [16], specifically designed for training transferable policies. The setting is based on a lightweight quadcopter platform known as Crazyflie 2.1¹ [17], which has been equipped with thrust upgraded motors and propellers. Finally, practical flying tests were conducted to validate the adaptation of the sim2real strategy. The preliminary results indicate that using a neural network, trained with reinforcement learning methods in a simulated environment, is both effective and feasible for comprehensive control of the drone.

¹Crazyflie 2.1: <https://www.bitcraze.io/products/crazyflie-2-1/>

The remainder of this article are organized in the following manner. Section 2. provides an overview of the methodologies including the quadcopter dynamics simulated environment, policy networks, and the training strategy. The experiments, involving the system’s configuration and the obtained results, are shown in section 3. Furthermore, in section 4., paper concludes by outlining potential future research and development opportunities.

2. METHODOLOGY

The diagram of end-to-end deep reinforcement learning quadcopter controller algorithm is demonstrated in Fig. 1. The quadcopter dynamics simulator is first established, followed by the designing of an actor-critic-based policy network that directly maps the states to the RPM commands of the motor. Quaternions are generally adopted to demonstrate orientation since they provide a global and compact expression. However, there is a specific drawback in our case, which is the existence of two figures that indicates the same rotation (i.e. $q = -q$). Therefore, we must either increase the amount of training data by two-fold or accept the issue of having a discontinuous function when we limit our domain to one hemisphere of S^3 . The rotation matrix is a representation that is highly redundant, but it is also simple and free from such issues. Hence, in order to eliminate the ambiguity that rose from the quaternion’s double coverage of the space of rotations, we convert them to a nine-element rotation matrix R .

Moreover, it is observed that the delay in the step-response is significant and is an effect of the low-pass behavior indicated by the motors. This behavior greatly affects the dynamics of the Crazyflie nano quadrotor used in this study. According to the manufacturer’s measurements², we have determined through empirical analysis that a time interval of 0.15 seconds would be sufficient for sim2real transference. These delays are considerably longer than the typical control interval of low-level controllers in Crazyflie. Therefore, they result in actions that affect the state only after 5 to 25 control steps [18]. In order to tackle the major amount of partial observability, we include the history of control actions into the observation. This is a proprioceptive measurement that can be easily done in software without the need of additional hardware. In addition, noise was introduced into the observation to imitate imperfections in the sensor feedback of the reality platform [18]. The unexpected noise values have a standard deviation of 0.001 for position and orientation, and 0.002 for linear velocity and angular velocity, respectively.

The observations are $18 + 4 \cdot N_{H_a}$ dimensional, where N_{H_a} is the number of action history [18], described as follows:

$$s_t = [p_t, R_t, v_t, \omega_t, H_a] \quad (1)$$

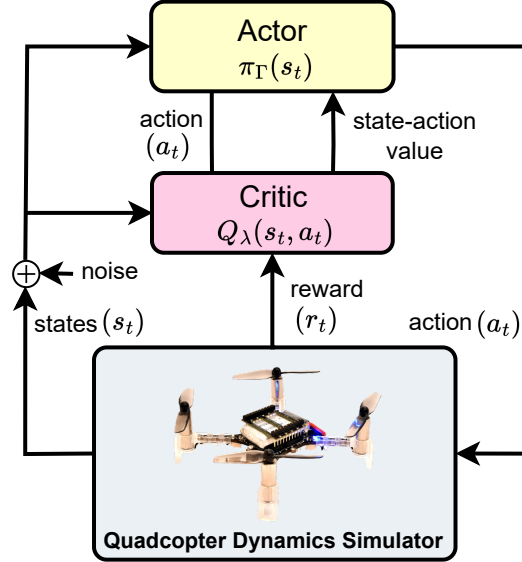


Fig. 1. Actor-critic-based end-to-end deep reinforcement learning quadcopter controller approach diagram.

where p_t denotes the position; R_t is the rotation matrix; v_t is linear velocity; ω_t is the angular velocity; H_a is the history of actions.

The actions comprise the RPM setpoints for each motor inside of the continuous space range of $[\min_a, \max_a]$ shown as below:

$$a_t = [r_1, r_2, r_3, r_4] = \pi_\Gamma(s_t) \quad (2)$$

2.1 Quadcopter dynamics simulator

We create a simulator that relies on the quadcopter dynamics model to train the policy network. In previous studies, a number of methods have been proposed and demonstrated to determine the dynamics model of the quadcopter using simulations and experiments [6, 7]. Let $\Xi = [\phi, \theta, \psi]^T \in \mathbb{R}^3$ denotes the quadcopter’s attitude including roll, pitch, and yaw angles in the Earth frame $\{E\}$ as shown in Fig. 2. The vehicle’s angular velocity in the body frame $\{B\}$ denoted as $\omega_b \in \mathbb{R}^3$. The position and velocity of the quadcopter along x, y, z-axis of $\{E\}$ are indicated by $p = [x, y, z]^T \in \mathbb{R}^3$, and $v = \dot{p}$, respectively. $J = \text{diag}(I_{xx}, I_{yy}, I_{zz}) \in \mathbb{R}^{3 \times 3}$ denotes the moment of inertia in $\{B\}$. The quadcopter’s dynamics model can be described by the following equations:

$$\omega_b = R(\Xi)\dot{\Xi} \quad (3)$$

$$m\dot{v} = mg + R(\Xi)u_3F_\Sigma \quad (4)$$

$$J\dot{\omega}_b = (J\omega_b) \times \omega_b + \tau \quad (5)$$

where m denotes the total mass of the quadcopter; $g \in \mathbb{R}^3$ is the gravitational acceleration vector; $u_3 = [0, 0, 1]^T$; F_Σ is the total thrust force; $R(\Xi)$ is the rotation matrix from $\{B\}$ to $\{E\}$, which is defined as:

$$R(\Xi) = \begin{bmatrix} 1 & 0 & -\sin(\theta) \\ 0 & \cos(\theta) & \sin(\phi)\cos(\theta) \\ 0 & -\sin(\theta) & \cos(\phi)\cos(\theta) \end{bmatrix} \quad (6)$$

²Crazyflie motor step response: <https://www.bitcraze.io/2015/02/measuring-propeller-rpm-part-3/>

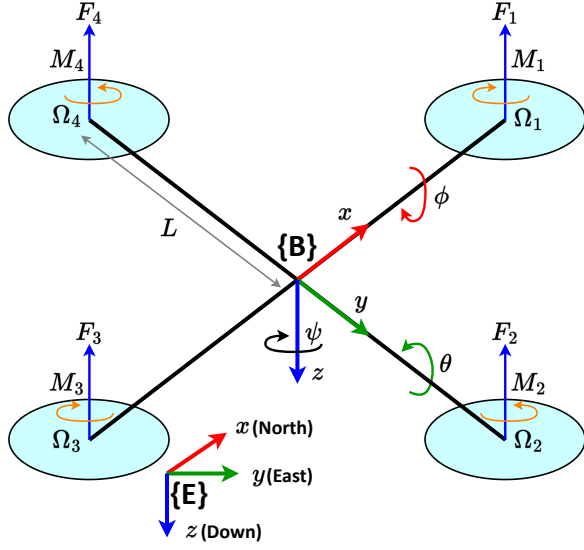


Fig. 2. The configuration of the quadcopter and coordinate systems with a body frame $\{B\}$ (x, y, z) and the Earth frame $\{E\}$ (N, E, D).

The control torque $\tau = [\tau_1, \tau_2, \tau_3]^T$ is generated by four propellers attached to four motors as follows:

$$\begin{cases} \tau_1 = LC_b(\Omega_2^2 - \Omega_4^2) \\ \tau_2 = LC_b(\Omega_3^2 - \Omega_1^2) \\ \tau_3 = C_d C_b(-\Omega_1^2 + \Omega_2^2 - \Omega_3^2 + \Omega_4^2) \end{cases} \quad (7)$$

where L represents the arm length of the quadcopter; Ω_i denotes the i -th motor's rotary speed ($i = 1, 2, 3, 4$); C_b and C_d consequently represent thrust and drag coefficient.

2.2 Networks architecture

We take advantage of the Twin Delayed Deep Deterministic policy gradient (TD3) [19], an off-policy reinforcement learning approach that provides enhanced sample complexity.

There are two networks, specifically a value network and a policy network, adopted for training. Both networks take the state as an input. We involve a fully-connected neural network to represent a policy. The policy network is formed by two hidden layers, each containing 64 neurons. The activation function employed in these layers is tanh, whereas the output layer uses linear activation. The value network has a same structure and is trained for predicting the state-action value function.

2.3 Rewards

For the initial state distribution, we sample uniformly from the following sets: The position is sampled inside a 0.2m box centered around the origin location. The orientation is represented by the rotation matrix R , which belongs to the entire $SO(3)$ group and has a maximum angle of 90 degrees. The linear velocity has a maximum magnitude of 1 m/s, while the angular velocity has a maximum value of 1 rad/s. In order to solve the issue of "learning to terminate" [20], we use a negative squared reward

function and includes an additional constant to encourage survival as follows:

$$r(s_t, a_t, s_{t+1}) = \lambda_s - \eta_p \|p_t\|_2^2 - \eta_R (1 - R_t^2) - \eta_v \|v_t\|_2^2 - \delta_a \|a_t - \delta_{ab}\|_2^2 \quad (8)$$

where λ_s is the survival bonus; η_p, η_R, η_v , and δ_a are the position, orientation, linear velocity, and action weights, respectively; δ_{ab} is the action baseline weight.

The survival bonus is configured with a high value in order to encourage the agent to maintain its life. The agent is penalized for deviating from the target state based on its position, orientation, linear velocity, and action terms. The position and orientation components have the highest cost coefficients due to their significant impact on the overall outcome. The other cost terms are chosen minimized to prevent the agent from executing unreasonable actions, which might result in crashing or straying from the desired state.

3. EXPERIMENTS

3.1 Systems Configurations

We verify our approach with the Bitcraze Crazyflie 2.1 quadcopter, which is equipped with the thrust improvement bundle package³. This kit includes longer 7×20 mm brushed coreless DC-motors and a 51MM-X2 propellers, resulting in enhanced agility as seen in Fig. 3b). The total weight of the assembled drone, which includes the batteries and reflective markers, is only 33 grams. This platform has a thrust-to-weight ratio slightly lower than 2 and utilizes an STM32F405 microcontroller operating at a clock speed of 168MHz. We use the pre-existing parameter estimates of the Crazyflie in [21] as illustrated in the Table 2.

The experiments were conducted in a $5 \times 4 \times 2.5$ m³ flying space at the Guidance, Navigation and Control Lab (GNC Lab) at Sejong University with the VICON Motion Capturing System consisting of 12 cameras as illustrated in Fig. 3a). It is assumed that we have access to actually precise estimates of the quadrotor's position, orientation, linear velocity, and angular velocity. The VICON system supplies the position and linear velocity data to a base station computer at a frequency of 100Hz, whereas the updates for orientation angle state estimate occur at 1kHz.

³<https://www.bitcraze.io/2022/10/thrust-upgrade-kit-for-the-crazyflie-2-1/>

Table 1. QUADCOPTER PARAMETERS USED FOR THE SIMULATOR.

Parameter	Value	Unit
m	0.033	kg
g	$[0, 0, -9.81]^T$	m/s ²
L	0.028	m
C_b	0.0059	Ns ²
C_d	9.18×10^{-7}	kg/rad
I_{xx}	16.57×10^{-6}	kgm ²
I_{yy}	16.66×10^{-6}	kgm ²
I_{zz}	29.26×10^{-6}	kgm ²

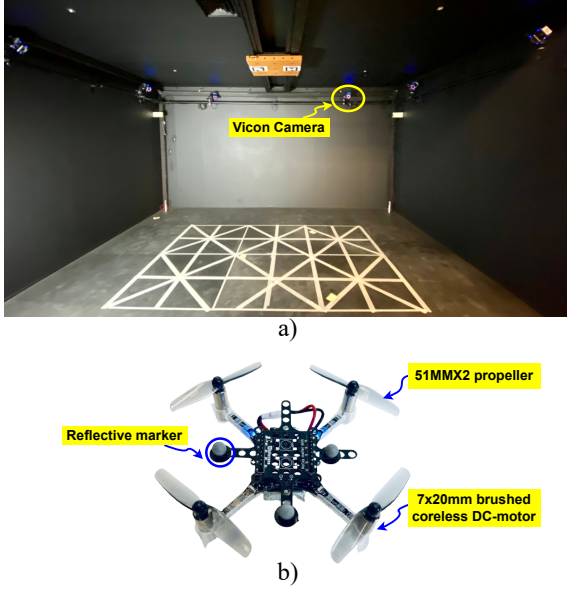


Fig. 3. Experimental conditions. a) VICON positioning system, b) Crazyflie 2.1 with thrust upgrade kit

The state estimate is obtained with an extended Kalman filter (EKF) [22] that combines data from the on-board IMU with motion capture information.

The control policy is a C-function that is automatically generated from the trained neural network model in PyTorch⁴. Next, we included the functionality to output the RPMs of all four motors in the Crazyflie firmware. The Crazyswarm API [23] is used to handle communication with the drone. The desired positions are sent to the quadrotor at a rate of 50Hz via a 2.4GHz radio dongle.

3.2 Experimental results

The training is conducted with the TD3 implementation in the Stable Baselines3 library [24]. We train the policy for a total of 5 million steps and takes slightly over 1 hours on a computer equipped Intel Core i9-13900K processor and NVIDIA 4090 GPU. The policy is trained with a batch size of 256, a learning rate of 10^{-3} . The length of the action history N_{H_a} is set to 32, the range action values is set as $[\min_a, \max_a]=[-21702, 27102]$. The values of rewards function parameters are specified in Table 2.

We evaluate the performance of our policy on the real Crazyflie quadrotor to follow a circle trajectory start at $x = 1$ and $y = 0$ with a radius of 1m in $T=6$ seconds. The formula of the circle trajectory is defined as:

⁴<https://pytorch.org/>

Table 2. PARAMETERS OF REWARDS FUNCTION.

Parameter	Value	Description
λ_s	2	Survival bonus
η_p	2.5	Position weight
η_R	2.5	Orientation weight
η_v	0.05	Linear velocity weight
δ_a	0.05	Action weight
δ_{ab}	0.35	Action baseline

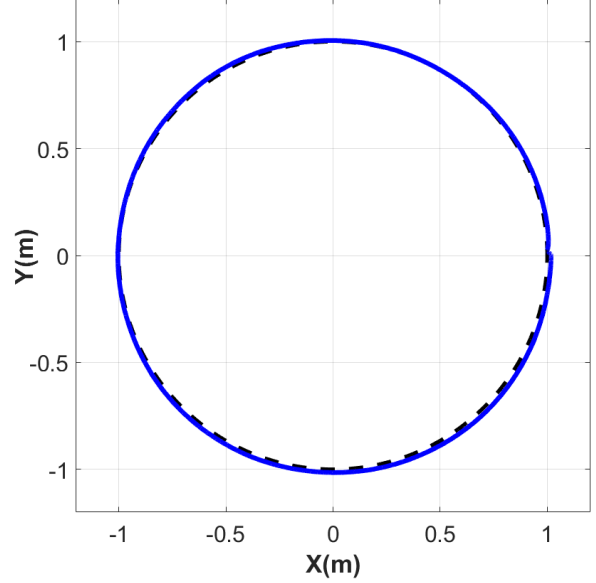


Fig. 4. Real flight tracking performance of circle trajectory with a radius of 1m in $T=6$ seconds.

$$p^d(t) = \begin{bmatrix} x_t^d \\ y_t^d \\ z_t^d \end{bmatrix} = \begin{bmatrix} 1 \\ 0 \\ 1 \end{bmatrix} = \begin{bmatrix} \cos(2\pi t/T) \\ \sin(2\pi t/T) \\ 0 \end{bmatrix} \quad (9)$$

where T is the cycle time.

The result of tracking performance is demonstrated in Fig. 4. There is a minor tracking error but it is not a significant amount. The trained policy is able to track circle trajectories in 6 seconds as in Fig. 5 where it reaches up to 1.8m/s. The real world experiments video can be found at: http://bit.ly/gnc_drl_quad_controller.

We compared our proposed approach with different traditional controllers, including Proportional-Integral-Derivative (PID) and Mellinger [25], utilizing same trajectory tracking task, hardware configuration, and Crazyswarm default gains. Compared to the other controllers our trained controller directly generates RPMs as output and hence does not take advantage battery voltage compensation, so we consider both the Root-Mean-Square Error (RMSE) with and without the z component as \bar{e} and \bar{e}_{xy} shown in Table 3, which are calculated as:

$$\bar{e} = \sqrt{\frac{1}{3} ((x - x^d)^2 + (y - y^d)^2 + (z - z^d)^2)} \quad (10)$$

$$\bar{e}_{xy} = \sqrt{\frac{1}{2} ((x - x^d)^2 + (y - y^d)^2)} \quad (11)$$

where x^d, y^d, z^d are the desired position, and x, y, z are the actual position.

Our controller policy has the capability of taking-off from the ground, which means overcoming the impact of near-ground airflow effects. While tracking the given trajectory, the Mellinger controller outperforms the PID controller due to the inclusion of an integral component, which aids in reducing steady state error.

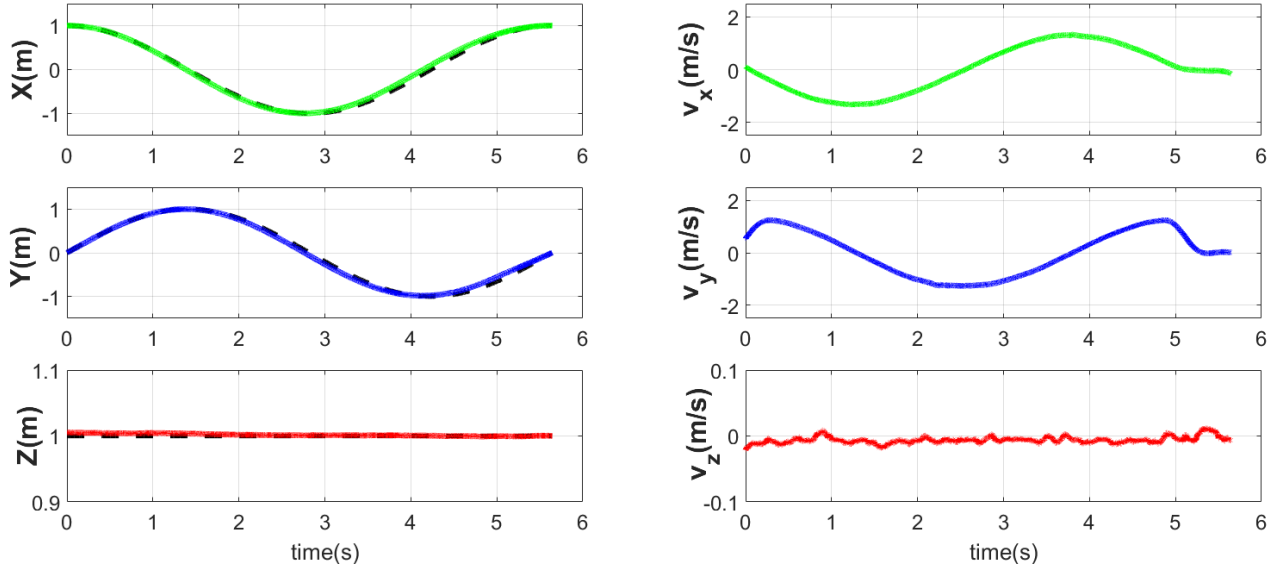


Fig. 5. Real flight tracking of a circle trajectory in the x, y, and z axes. Left: position tracking performance; Right: linear velocity tracking performance.

Table 3. Comparison of tracking error when tracking the circle trajectory of different controllers.

Controller	Tracking error (m)	
	\bar{e}	\bar{e}_{xy}
PID	0.68	0.67
Mellinger [25]	0.18	0.18
Ours	0.18	0.16

Although our policy does not have integral part memory, but it is equivalent to the Mellinger controller in terms of distance with 0.18m and has a smaller error in the xy-plane with 0.16m.

4. CONCLUSION

This research presents a reinforcement learning scheme for a quadrotor controller that generates RPMs directly based on the vehicle’s states. Once trained with the simulator on a computer, the policy is directly utilized on real-world Crazyflie platforms for carrying out real flying tests in the VICON positioning system, without necessity for expert parameter adjustments. The presented technique has been evaluated by experimental results, which indicate its efficiency and practicality. The trained policy is able of operating onboard and demonstrates precise trajectory tracking capabilities.

There are still potential to further development in order to achieve even more outstanding results. In future works, it is essential to enhance the robustness by extending the policy to take into account the changes in system parameters or environmental disturbances, such as variations in battery levels or wind gusts.

REFERENCES

- [1] T.-D. Do, N. Xuan-Mung, H. Jeong, Y.-S. Lee, C.-W. Sung, and S. K. Hong, “Vision-based autonomous perching of quadrotors on horizontal surfaces,” in *2023 International Conference on System Science and Engineering (ICSSE)*, pp. 352–357, IEEE, 2023.
- [2] L.-A. Tran, N.-P. Le, T.-D. Do, and M.-H. Le, “A vision-based method for autonomous landing on a target with a quadcopter,” in *2018 4th International Conference on Green Technology and Sustainable Development (GTSD)*, pp. 601–606, IEEE, 2018.
- [3] T.-D. Do, N. Xuan-Mung, N.-P. Nguyen, J.-W. Lee, Y.-S. Lee, S.-T. Lee, and S.-K. Hong, “Multi-sensor-based target pose estimation for autonomous precision perching of nano aerial vehicles,” in *2022 22nd International Conference on Control, Automation and Systems (ICCAS)*, pp. 1565–1571, IEEE, 2022.
- [4] Y. Wang, W. Liu, J. Liu, and C. Sun, “Cooperative usv-uav marine search and rescue with visual navigation and reinforcement learning-based control,” *ISA transactions*, vol. 137, pp. 222–235, 2023.
- [5] M. Lyu, Y. Zhao, C. Huang, and H. Huang, “Unmanned aerial vehicles for search and rescue: A survey,” *Remote Sensing*, vol. 15, no. 13, p. 3266, 2023.
- [6] N. Xuan-Mung, N. P. Nguyen, D. B. Pham, N.-N. Dao, H. T. Nguyen, T. Ha Le Nhu Ngoc, M. T. Vu, and S. K. Hong, “Novel gain-tuning for sliding mode control of second-order mechanical systems: theory and experiments,” *Scientific Reports*, vol. 13, no. 1, p. 10541, 2023.
- [7] T.-D. Do, N. Xuan-Mung, Y.-S. Lee, and S. K. Hong, “An efficient fixed-time filter for backstepping attitude control of quadcopter,” in *2023 9th International Conference on Control, Decision and Information Technologies (CoDIT)*, pp. 2151–2157, IEEE, 2023.
- [8] S. Kuutti, R. Bowden, Y. Jin, P. Barber, and S. Fallah, “A survey of deep learning applications to autonomous vehicle control,” *IEEE Transactions on*

Intelligent Transportation Systems, vol. 22, no. 2, pp. 712–733, 2020.

- [9] T.-D. Do, M.-T. Duong, Q.-V. Dang, and M.-H. Le, “Real-time self-driving car navigation using deep neural network,” in *2018 4th International Conference on Green Technology and Sustainable Development (GTSD)*, pp. 7–12, IEEE, 2018.
- [10] T. P. Lillicrap, J. J. Hunt, A. Pritzel, N. Heess, T. Erez, Y. Tassa, D. Silver, and D. Wierstra, “Continuous control with deep reinforcement learning,” *arXiv preprint arXiv:1509.02971*, 2015.
- [11] J. Schulman, P. Moritz, S. Levine, M. Jordan, and P. Abbeel, “High-dimensional continuous control using generalized advantage estimation,” *arXiv preprint arXiv:1506.02438*, 2015.
- [12] J. Schulman, F. Wolski, P. Dhariwal, A. Radford, and O. Klimov, “Proximal policy optimization algorithms,” *arXiv preprint arXiv:1707.06347*, 2017.
- [13] J. Hwangbo, I. Sa, R. Siegwart, and M. Hutter, “Control of a quadrotor with reinforcement learning,” *IEEE Robotics and Automation Letters*, vol. 2, no. 4, pp. 2096–2103, 2017.
- [14] A. Molchanov, T. Chen, W. Hönig, J. A. Preiss, N. Ayanian, and G. S. Sukhatme, “Sim-to-(multi)-real: Transfer of low-level robust control policies to multiple quadrotors,” in *2019 IEEE/RSJ International Conference on Intelligent Robots and Systems (IROS)*, pp. 59–66, IEEE, 2019.
- [15] K. Huang, R. Rana, A. Spitzer, G. Shi, and B. Boots, “Datt: Deep adaptive trajectory tracking for quadrotor control,” *arXiv preprint arXiv:2310.09053*, 2023.
- [16] G. Brockman, V. Cheung, L. Pettersson, J. Schneider, J. Schulman, J. Tang, and W. Zaremba, “Openai gym,” *arXiv preprint arXiv:1606.01540*, 2016.
- [17] W. Giernacki, M. Skwierczyński, W. Witwicki, P. Wroński, and P. Kozierski, “Crazyflie 2.0 quadrotor as a platform for research and education in robotics and control engineering,” in *2017 22nd International Conference on Methods and Models in Automation and Robotics (MMAR)*, pp. 37–42, IEEE, 2017.
- [18] J. Eschmann, D. Albani, and G. Loianno, “Learning to fly in seconds,” *IEEE Robotics and Automation Letters*, vol. 9, no. 7, pp. 6336–6343, 2024.
- [19] S. Fujimoto, H. Hoof, and D. Meger, “Addressing function approximation error in actor-critic methods,” in *International conference on machine learning*, pp. 1587–1596, PMLR, 2018.
- [20] J. Eschmann, “Reward function design in reinforcement learning,” *Reinforcement learning algorithms: Analysis and Applications*, pp. 25–33, 2021.
- [21] J. Forster, “System identification of the crazyflie 2.0 nano quadcopter,” *PhD thesis*, 2015.
- [22] R. E. Kalman, “A new approach to linear filtering and prediction problems,” 1960.
- [23] J. A. Preiss, W. Honig, G. S. Sukhatme, and N. Ayanian, “Crazyswarm: A large nano-quadcopter swarm,” in *2017 IEEE International Conference on Robotics and Automation (ICRA)*, pp. 3299–3304, IEEE, 2017.
- [24] A. Raffin, A. Hill, A. Gleave, A. Kanervisto, M. Ernestus, and N. Dormann, “Stable-baselines3: Reliable reinforcement learning implementations,” *Journal of Machine Learning Research*, vol. 22, no. 268, pp. 1–8, 2021.
- [25] D. Mellinger and V. Kumar, “Minimum snap trajectory generation and control for quadrotors,” in *2011 IEEE International Conference on Robotics and Automation*, pp. 2520–2525, IEEE, 2011.